Available online at www.sciencedirect.com

SCIENCE DIRECT

Diamond & Related Materials 14 (2005) 1432 – 1443

DIAMOND AND RELATED MATERIALS

www.elsevier.com/locate/diamond

Analysis of carbon nitride growth in pedestal reactors by chemical vapor deposition

Jungheum Yun*, David S. Dandy

Department of Chemical Engineering, Colorado State University, Fort Collins, CO, USA

Received 18 October 2002; received in revised form 17 February 2005; accepted 18 February 2005
Available online 6 May 2005

Abstract

The chemical vapor deposition of polycrystalline carbon nitride in stagnation flow reactors is simulated. A model is used to predict the gas phase chemistry, temperature and velocity profiles, potential gaseous film growth precursors, and to evaluate the likelihood of bond rearrangement occurring in the bulk phase or on the deposition surface once the gaseous precursors are adsorbed. Numerical studies are carried out to predict the effects of inlet and substrate temperatures, reactor pressure, and inlet gas composition on the gas phase chemistry. Potential gaseous film growth precursors of carbon nitride are determined by quantitatively comparing the calculated results against existing experimental data. Results of the model indicate that the gas phase chemistry, including the gas composition at the deposition surface, is strongly affected by reactor pressure and inlet gas composition. However, the gas composition at the deposition surface does not depend strongly on the inlet temperature, while it is found to be strongly dependent on the substrate temperature. Since no correlation is found between the predicted near-surface concentrations of potential film growth precursors and experimentally measured bond types in the carbon nitride films, the experimentally measured bond types in the films must therefore result from chemical bond rearrangement occurring on the deposition surface or in the bulk phase once the gaseous precursors are adsorbed. Comparison between the calculated film growth rate using potential growth precursors and experimental data indicates that the CH_x ($x=0,2,3$), C_2H_2, NH_x ($x=0,1,2$), and H_xCN ($x=1,2$) species are the most probable crystalline carbon nitride growth species. Among these, C and CH_3 dominate the carbon contribution to the film growth, and N is the primary nitrogen bearing species responsible for the film growth. The sum of predicted film growth rates for carbon bearing species is comparable to the experimentally determined film growth rate.

Keywords: Carbon nitride; Chemical vapor deposition; Simulation

1. Introduction

Liu and Cohen [1,2] have predicted that β-C_3N_4, a polytype of crystalline carbon nitride (C−N), would have a hardness comparable to or greater than that of diamond. The postulation was based on a combination of an empirical model [1] and an ab initio calculation [2], indicating that a large bulk modulus could be achieved for a covalent solid formed between carbon and nitride with short covalent bond lengths and low ionicity. The material is expected to have a structure similar to that of β-Si_3N_4, with carbon replacing the silicon in a network of CN_4 tetrahedra linked at the corners. Its structure would be sp^3 hybridized at carbon and sp^2 hybridized at nitrogen [2].

The theoretical prediction of Liu and Cohen was supported by a local density approximation-based (LDA) calculation for the structural and electronic properties of β-C_3N_4 [3]. The LDA calculation indicated that β-C_3N_4 might be an energetically favorable phase in the C−N solid because the cohesive energy of β-C_3N_4 was predicted to be moderately large, 81.5 eV/unit cell. It was also predicted that two metastable structures, one resembling a zinc-blende CN vacancy per cubic cell and the other resembling graphitic CN with one C vacancy per four N sites, could be synthesized

* Corresponding author. Present address: Power Electronic Research Center, National Institute of Advanced Industrial Science and Technology (AIST), Tsukuba, Ibaraki, 305-8568, Japan. Tel.: +81 29 861 9177; fax: +81 29 861 5434.
E-mail address: jungheum.yun@aist.go.jp (J. Yun).

0925-9635/$ - see front matter © 2005 Elsevier B.V. All rights reserved.
doi:10.1016/j.diamond.2005.02.011

in addition to the hexagonal β-C_3N_4 structure [3,4]. According to that study, both the refined β-phase and the cubic phase would also have compressibilities comparable to that of diamond (1.7×10^{-7} cm^2/kg), where the compressibility of diamond is lower than any known material.

However, Guo and Goddard [5] produced a theoretical result contradicting the hypothesis of Liu and Cohen [1–4]. Guo and Goddard's prediction of the crystalline properties of C_3N_4 was based on the method of molecular simulation force field (MSFF). They pointed out the restrictions within the calculation carried out by Liu and Cohen [2,3] that led to different quantitative results. It was concluded by Guo and Goddard that, in the earlier calculations, the bulk modulus of C_3N_4 was over-predicted because the possibility of nonplanar nitrogen in the C_3N_4 structure was not considered and a uniform scale in the coordinate system was assumed. The results of Guo and Goddard indicated that α-C_3N_4 would be more stable than β-C_3N_4 due to the large energy difference between these phases. Thus, according to Guo and Goddard, a carbon nitride film formed with thin film deposition techniques would be α-C_3N_4. In addition, they predicted that the bulk modulus of α- and β-C_3N_4 would be about half the value for diamond and, surprisingly, that the Poisson ratio of α-C_3N_4 would be negative.

Despite the predictions of Guo and Goddard [5] to the contrary, in the last several years there have been considerable efforts to synthesize and analyze β-C_3N_4 films [6–20]. Most investigators have observed the formation of amorphous carbon films containing varying amounts of nitrogen, generically referred to as CN_x. The synthesis of crystalline β-C_3N_4 in amorphous CN_x films has been reported in only several cases [12–20]. Film deposition techniques in these investigations have included pulsed laser ablation [12], radio frequency (rf) [13,18] and plasma arc sputtering [14], chemical vapor deposition (CVD) [15,16,20], shock wave compression [17], and ion-assisted deposition [19]. It is important to note that, while these investigators all report the existence of nano- or micro-crystals of β-C_3N_4 within an amorphous matrix, others who have studied this material do not view the evidence as sufficiently conclusive. For example, in critical reviews of carbon nitride research [21,22], potential issues in experimental methodology or characterization have been highlighted. These reviews do not preclude the possibility of synthesizing crystalline C_3N_4; rather, they point out the challenges to be addressed.

Most experimental investigations into the growth of β-C_3N_4, which have used a mixture of CH_4 and N_2 as the feed, indicate that the CN_x films have much lower nitrogen concentration than the 57% required for stoichiometric C_3N_4. This result suggests that very high concentrations of reactive nitrogen bearing gaseous species, including atomic nitrogen, are necessary for the growth of C_3N_4 [15]. Among the various low pressure film deposition techniques attempted thus far, CVD is an attractive method for the β-C_3N_4 synthesis because of its precise control of gas composition and high incident surface flux of reactive gaseous species. Studies on the synthesis of β-C_3N_4 have been conducted using techniques similar to those used in diamond CVD, with the addition of a nitrogen component [20]. Zhang et al. [20] reported that crystalline carbon nitride films with large crystalline grains, up to ~10 μm in size, and film-like regions of the crystalline phase were grown on polycrystalline Ni substrates using a plasma-assisted hot filament chemical vapor deposition technique. They concluded that the crystallographic structure associated with β-C_3N_4 was present in the deposited films based upon X-ray diffraction (XRD) spectra. Unfortunately, adequate samples for quantitative measurements of the bulk modulus of the crystalline carbon nitride have not yet been synthesized. However, it may be possible to determine the crystal structure, stability of β-C_3N_4, and other metastable carbon nitride phases if thicker, higher quality films of crystalline carbon nitride can be deposited on substrates. High quality crystalline carbon nitride may be synthesized using thin film techniques if a more thorough understanding of carbon nitride deposition conditions is achieved.

A detailed theoretical analysis of the elementary surface reactions leading to carbon nitride growth has not yet been reported, and the task of uncovering these mechanisms may prove to be difficult. However, if the goal is limited to predicting the growth rate of the carbon nitride film, relatively few surface reactions – including reactions of probable gaseous film growth precursors with surface reactive sites, H-atom abstraction, and surface reactive site termination – will describe the features of interest. Further, the growth rate can be maximized if the near-surface concentrations of the most probable gaseous film growth precursors are maximized. This can only be achieved by identifying probable growth precursors. Probable growth precursors of carbon nitride may be identified by examining mass fluxes of gaseous species at the deposition surface using simplified growth mechanisms and comparing these to experimentally determined deposition rates. In addition, the availability of data describing the relative concentrations of different bond types (C–N, C=N, C≡N, C=C, etc.) in solid CN_x films [7] provides the opportunity to explore the extent to which bond rearrangement occurs on the deposition surface or in the bulk phase once reactive species are adsorbed. Put another way, since CN_x films grown to date do not exhibit exclusive sp^2 hybridization for nitrogen and sp^3 hybridization for carbon, it is useful to ask whether these films inherit their spectrum of bond types directly from the species adsorbing from the gas phase, or by subsequent chemical rearrangement of the bonds after the molecules have been adsorbed. This issue can be investigated by examining whether the predicted fluxes of gaseous species at the surface correlate with the relative concentrations of bond types in the films.

The results of two experimental studies by Ricci et al. [7] and Zhang et al. [20] are compared to the predictions in this study. Although there have been a number of attempts to synthesize C_3N_4 via CVD, detailed data on the deposition

rate of the carbon nitride film and the relative concentrations of different bond types in the films are not readily available in the literature.

The primary purposes of this study are to explore the gas phase chemistry and its dependence on operating conditions, temperature and velocity profiles, and to determine potential gaseous film growth precursors of carbon nitride film deposition occurring inside pedestal stagnation flow CVD reactors. It is not the intent of this study to prove or disprove the existence of β-C_3N_4. The focus will be on the details of the chemistry occurring during CVD growth of carbon nitride. Indeed, as will be shown, the model supports observations that CN_x films are invariably deficient in nitrogen. In addition, it is worthwhile exploring whether significant bond rearrangement occurs on the deposition surface or in the bulk phase once the gaseous precursors are adsorbed because this may give some indication of the possible complexity of quantitative deposition models. The governing conservation equations, including gas phase and surface reactions, are solved numerically to simulate these aspects of carbon nitride film growth.

In the examination of both probable growth precursors and bond type correlation, a simplified set of surface reactions is applied to obtain mass fluxes of gaseous species at the deposition surface. The collision and subsequent surface reaction of a gaseous species with the deposition surface results in the formation of a surface species; bulk species are then formed when all reactive bonds of a surface species are to other surface species or bulk species through surface reactions. The surface reactions are considered as irreversible, and the rate constants are represented by sticking probabilities.

First, the CVD system under study is described, and the corresponding governing equations and boundary conditions are discussed. The experimental data of Ricci et al. [7] is used to see whether a correlation exists between bond types of adsorbing species and bond types in the carbon nitride films. The film growth rate is calculated for each presumed growth precursor using the experimental operating conditions of Zhang et al. [20]. Then, comparisons between the computational results and experimental data are used to predict the possible gaseous species contributing to the growth of carbon nitride. Finally, the numerical model is applied to investigate the effects of various operating parameters – the inlet and substrate temperatures, reactor pressure, and inlet gas composition – on the concentrations of probable growth precursors at the deposition surface. The operating conditions to be used are selected from existing experimental data on carbon nitride growth via CVD.

2. Model description

Consider a system configured with the inlet axis orthogonal to the substrate such that a forced flow of reactant gases impinges upon an isothermal substrate, as illustrated in Fig. 1. The geometry of the system is described in terms of cylindrical coordinates (r, ϕ, z), with the origin of the coordinate system located at the center on the substrate surface. An idealized stagnation flow geometry is assumed to exist in the region between the inlet and the substrate. The gas flows uniformly downward from the inlet towards the substrate surface with known temperature, velocity, and composition at the inlet. The uniform axial down flow at inlet, located at the position $z=L$, is given by $-U_\infty$, and the temperature and mole fractions at this location are denoted by T_∞ and $X_{k\ \infty}$. The axial velocity component does not vanish at the substrate surface due to the net deposition of mass onto that surface. The radial velocity component at the surface vanishes due to the no-slip condition. At the deposition surface the gas temperature matches that of the substrate, T_s. At steady state the net production rate of a gaseous species at the substrate surface is equal to its mass flux at the substrate surface, and the net production rate of any surface species on the substrate surface is zero.

The steady-state conservation equations describe the momentum and energy transport, convective and diffusive transport of the species, the chemical composition of the gas phase, and the surface concentrations of the adsorbed species [23,24]. The conservation equations consist of radial, axial, and circumferential momentum equations, gaseous species continuity equations, a mixture continuity equation, thermal energy equation, and surface species conservation equations. The conservation equations yield an axisymmetric similarity solution for the geometry shown in Fig. 1 because all dependent variables in the equations may be considered to be functions only of axial coordinate, z, with radial and angular velocities rescaled by the radial coordinate, r [25]. The conservation

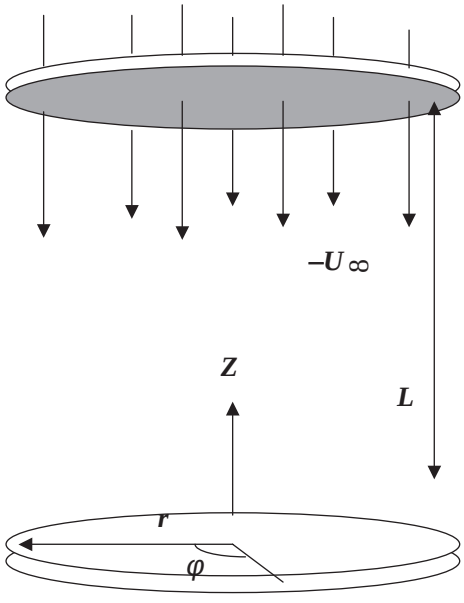

Fig. 1. Schematic diagram of the CVD geometry considered. The geometry of the system is represented in terms of the cylindrical coordinates (r, ϕ, z).

Table 1
Gas-phase reaction mechanisms

Reaction		A_i[a]	b_i[a]	E_i[a]
G1	$H+H+M \leftrightarrow H_2+M$	0.100×10^{19}	−1.0	0.0
G2	$H+H+H_2 \leftrightarrow H_2+H_2$	0.920×10^{17}	−0.6	0.0
G3	$CH_3+CH_3(+M) \leftrightarrow C_2H_6(+M)$	9.220×10^{16}	−1.174	635.8
G4	$CH_3+H(+M) \leftrightarrow CH_4(+M)$	6.000×10^{16}	−1.0	0.0
G5	$CH_4+H \leftrightarrow CH_3+H_2$	0.220×10^{5}	3.0	8750.0
G6	$CH_3+H \leftrightarrow CH_2+H_2$	0.900×10^{14}	0.0	15 100.0
G7	$CH_2+H \leftrightarrow CH+H_2$	0.100×10^{19}	−1.56	0.0
G8	$CH+H \leftrightarrow C+H_2$	0.150×10^{15}	0.0	0.0
G9	$CH+CH_2 \leftrightarrow C_2H_2+H$	0.400×10^{14}	0.0	0.0
G10	$CH+CH_3 \leftrightarrow C_2H_3+H$	0.300×10^{14}	0.0	0.0
G11	$CH+CH_4 \leftrightarrow C_2H_4+H$	0.600×10^{14}	0.0	0.0
G12	$C+CH_3 \leftrightarrow C_2H_2+H$	0.500×10^{15}	0.0	0.0
G13	$C+CH_2 \leftrightarrow C_2H+H$	0.500×10^{14}	0.0	0.0
G14	$C_2H_6+CH_3 \leftrightarrow C_2H_5+CH_4$	0.550×10^{0}	4.0	8300.0
G15	$C_2H_6+H \leftrightarrow C_2H_5+H_2$	0.540×10^{3}	3.5	5210.0
G16	$C_2H_4+H \leftrightarrow C_2H_3+H_2$	5.420×10^{14}	0.0	14 902.0
G17	$CH_2+CH_3 \leftrightarrow C_2H_4+H$	0.400×10^{14}	0.0	0.0
G18	$H+C_2H_4\ (+M) \leftrightarrow C_2H_5\ (+M)$	0.221×10^{14}	0.0	2066.0
G19	$C_2H_5+H \leftrightarrow CH_3+CH_3$	1.000×10^{14}	0.0	0.0
G20	$H_2+C_2H \leftrightarrow C_2H_2+H$	0.409×10^{6}	2.39	864.3
G21	$H+C_2H_2\ (+M) \leftrightarrow C_2H_3\ (+M)$	0.554×10^{13}	0.0	2410.0
G22	$C_2H_3+H \leftrightarrow C_2H_2+H_2$	0.400×10^{14}	0.0	0.0
G23	$C_2H_3+C_2H \leftrightarrow C_2H_2+C_2H_2$	0.300×10^{14}	0.0	0.0
G24	$C_2H_3+CH \leftrightarrow CH_2+C_2H_2$	0.500×10^{14}	0.0	0.0
G25	$CH_2(S)+M \leftrightarrow CH_2+M$	0.100×10^{14}	0.0	0.0
G26	$CH_2(S)+CH_4 \leftrightarrow CH_3+CH_3$	0.400×10^{14}	0.0	0.0
G27	$CH_2(S)+C_2H_6 \leftrightarrow CH_3+C_2H_5$	0.120×10^{15}	0.0	0.0
G28	$CH_2(S)+H_2 \leftrightarrow CH_3+H$	0.700×10^{14}	0.0	0.0
G29	$CH_2(S)+C_2H_2 \leftrightarrow CH_2+C_2H_2$	4.0×10^{13}	0.0	0.0
G30	$CH_2(S)+H \leftrightarrow CH_2+H$	0.200×10^{15}	0.0	0.0
G31	$CH_2(S)+H \leftrightarrow CH+H_2$	3.000×10^{13}	0.0	0.0
G32	$CH_2(S)+CH_3 \leftrightarrow C_2H_4+H$	2.000×10^{13}	0.0	0.0
G33	$C_2+H_2 \leftrightarrow C_2H+H$	4.0×10^{5}	2.4	1000.0
G34	$CH_2+CH_2 \leftrightarrow C_2H_2+H+H$	0.400×10^{14}	0.0	0.0
G35	$C_2H_2+M \leftrightarrow C_2H+H+M$	0.420×10^{17}	0.0	10 700.0
G36	$C_2H_4+M \leftrightarrow C_2H_2+H_2+M$	0.150×10^{16}	0.0	55 800.0
G37	$C_2H_4+M \leftrightarrow C_2H_3+H+M$	0.140×10^{17}	0.0	82 360.0
G38	$CH+N_2 \leftrightarrow HCN+N$	5.400×10^{12}	0.0	25 000.0
G39	$C+N_2 \leftrightarrow CN+N$	6.300×10^{13}	0.0	46 019.0
G40	$CH_2+N_2 \leftrightarrow HCN+NH$	0.100×10^{14}	0.0	74 000.0
G41	$H_2CN+N \leftrightarrow N_2+CH_2$	0.200×10^{14}	0.0	0.0
G42	$H_2CN+M \leftrightarrow HCN+H+M$	0.300×10^{15}	0.0	22 000.0
G43	$CH_2+N \leftrightarrow HCN+H$	0.500×10^{14}	0.0	0.0
G44	$CH+N \leftrightarrow CN+H$	0.130×10^{14}	0.0	0.0
G45	$CH_3+N \leftrightarrow H_2CN+H$	7.100×10^{13}	0.0	0.0
G46	$C_2H_3+N \leftrightarrow HCN+CH_2$	0.200×10^{14}	0.0	0.0
G47	$CN+H_2 \leftrightarrow HCN+H$	0.295×10^{6}	2.45	2237.0
G48	$CH+HCN \leftrightarrow CH_2+CN$	3.010×10^{13}	0.0	−993.5
G49	$CN+HCN \leftrightarrow C_2N_2+H$	1.320×10^{3}	2.7	646.0
G50	$CN+CH_4 \leftrightarrow CH_3+HCN$	6.020×10^{4}	2.64	−437.0
G51	$CN+C_2H_6 \leftrightarrow C_2H_5+HCN$	1.200×10^{5}	2.77	−1788.0
G52	$NCN+H \leftrightarrow HCN+N$	1.000×10^{14}	0.0	0.0
G53	$NH+N \leftrightarrow N_2+H$	0.300×10^{14}	0.0	0.0
G54	$NH+H \leftrightarrow N+H_2$	3.000×10^{13}	0.0	0.0
G55	$NH_2+H \leftrightarrow NH+H_2$	0.692×10^{14}	0.0	3650.0
G56	$NH_3+H \leftrightarrow NH_2+H_2$	0.636×10^{6}	2.39	10 171.0
G57	$NNH \leftrightarrow N_2+H$	1.000×10^{6}	0.0	0.0
G58	$NNH+H \leftrightarrow N_2+H_2$	0.100×10^{15}	0.0	0.0
G59	$NNH+NH_2 \leftrightarrow N_2+NH_3$	0.500×10^{14}	0.0	0.0
G60	$NNH+NH \leftrightarrow N_2+NH_2$	0.500×10^{14}	0.0	0.0
G61	$NH_2+NH \leftrightarrow N_2H_2+H$	0.500×10^{14}	0.0	0.0
G62	$NH+NH \leftrightarrow N_2+H+H$	0.254×10^{14}	0.0	0.0
G63	$NH_2+N \leftrightarrow N_2+H+H$	0.720×10^{14}	0.0	0.0
G64	$N_2H_2+M \leftrightarrow NNH+H+M$	0.500×10^{17}	0.0	50 000.0
G65	$N_2H_2+H \leftrightarrow NNH+H_2$	0.500×10^{14}	0.0	1000.0
G66	$N_2H_2+NH \leftrightarrow NNH+NH_2$	0.100×10^{14}	0.0	1000.0
G67	$N_2H_2+NH_2 \leftrightarrow NH_3+NNH$	0.100×10^{14}	0.0	1000.0
G68	$NH_2+NH_2 \leftrightarrow N_2H_2+H_2$	0.500×10^{12}	0.0	0.0

[a] Arrhenius parameters for the forward reaction rate constants shown in the form $k_{fi}=A_i T^{b_i} e^{-E_i/RT}$ (A_i in moles, cubic centimeters, and seconds; E_i in cal/mol). Each of the gas-phase reactions is reversible, and the reverse rate is obtained from the reaction equilibrium constants. All reaction rates, equilibrium constants, and thermodynamic properties for gas-phase species are evaluated by using Chemkin-III [26].

equations are comprised of K_g+K_s+4 coupled ordinary differential equations, together with the necessary constitutive equations and boundary conditions, where K_g and K_s are the numbers of gaseous species and surface species in the model, respectively.

Numerical solutions for the governing equations and the appropriate boundary conditions are found for the gas composition, temperature and velocity profiles, and deposition rates [23]. Chemkin-III, a Fortran chemical kinetics package, is used for the analysis of gas phase chemical kinetics [26]. The gas phase reaction mechanism used in this study is listed in Table 1 [27]. The reaction mechanism for C/N/H gas mixtures has been also reported in other kinetic studies [28–30], but the predicted gas phase chemistry from the mechanism used in this study [27] is in a reasonable agreement with those from other mechanisms. The gas-phase multicomponent transport properties are evaluated

Table 2
Surface reaction mechanisms for presumed film growth precursors

Growth species		Reaction
CH_x	S1	$NH(S)+H \rightarrow N^*(S)+H_2$
	S2	$N^*(S)+H \rightarrow NH(S)$
$(x\neq0)$	S3	$N^*(S)+CH_x \rightarrow B+CH(S)+H_{x-1}$
or (x=0)	S3	$N^*(S)+C \rightarrow B+C^*(S)$
C_2H_x	S4	$NH(S)+H \rightarrow N^*(S)+H_2$
	S5	$N^*(S)+H \rightarrow NH(S)$
	S6	$N^*(S)+C_2H_x \rightarrow B+C_2H(S)+H_{x-1}$
NH_x	S7	$CH(S)+H \rightarrow C^*(S)+H_2$
	S8	$C^*(S)+H \rightarrow CH(S)$
(x≠0)	S9	$C^*(S)+NH_x \rightarrow B+NH(S)+H_{x-1}$
or (x=0)	S9	$C^*(S)+N \rightarrow B+N^*(S)$
H_xCN	S10	$NH(S)+H \rightarrow N^*(S)+H_2$
	S11	$N^*(S)+H \rightarrow NH(S)$
	S12	$N^*(S)+H_xCN \rightarrow B+HCN(S)+H_{x-1}$
or	S13	$CH(S)+H \rightarrow C^*(S)+H_2$
	S14	$C^*(S)+H \rightarrow CH(S)$
	S15	$C^*(S)+H_xCN \rightarrow B+HCN(S)+H_{x-1}$

The surface sites and bulk species are represented by S and B. Each of the surface reactions is irreversible, and the sticking coefficients γ_i are used to convert surface reaction rate constants. The sticking coefficient's form for reaction i is taken to be $\gamma_i=a_i T^{B_i} e^{-c_i/RT}$ where a_i and B_i are unitless and c_i has units compatible with the gas constant R. Because γ_i is defined as a probability, it must lie between 0 and 1. Equilibrium constants and thermodynamic properties for surface reactions are evaluated by using Surface Chemkin [32].

using a computer package [31]. Surface Chemkin is used for the treatment of the heterogeneous reactions occurring at the deposition surface and these are listed in Table 2 [32].

3. Results and discussion

Calculations are carried out to determine the gaseous species most likely to lead to the growth of carbon nitride, and to investigate whether significant bond rearrangement occurs once the gaseous precursors are adsorbed. Operating conditions are chosen to facilitate comparison with two existing experiments [7,20]. Probable gaseous film growth precursors are determined by examining which calculated mass fluxes due to presumed growth precursors could account for the observed growth rate. The extent of bond rearrangement is investigated by inspecting whether the calculated mass fluxes at the deposition surface correlate with the experimentally measured reactive concentrations of bond types in the solid films. Further, once the probable growth precursors are determined, the effects of operating parameters – the inlet and substrate temperatures, reactor pressure, and inlet gas composition – on the concentrations of probable growth precursors at the deposition surface are investigated.

3.1. Correlation between gas and solid bond types

Ricci et al. [7] used IR absorption to measure several different chemical bond types, including C=N, C=C, C−N, N−H, and C≡N, in CN_x films grown using a rf plasma assisted CVD reactor. In the present calculations, the relative concentrations of the bond types in the films are determined from the absorbance measurements of Ricci et al. using Beer's law, which describes the direct proportionality between the absorbance and concentration, and these are found to be (C=N:C=C:C−N:N−H:C−H:C≡N)=(9:9:7.5:6.5:6.5:6.3–6.4). The existence of the C≡N bond in carbon nitride films was reported by Ogata et al. [8] and Krishna et al. [11]. Diani et al. [9] detected large numbers of C−N and C=N bonds in synthesized carbon nitride films. Bousetta et al. [10] observed the existence of NH_2, C−N, CH, C≡N, and CH_2 bonds in their carbon nitride films. Thus, it appears that C≡N, C=N, and C−N bonds are common in CN_x films grown to date.

Table 3
Experimental conditions of Ricci et al. used in the model

Reactor pressure P (torr)		0.75
Inlet gas temperature T_∞ (K)		300
Substrate temperature T_s (K)		300
rf excitation power (W)		100[a]
Inlet mole fractions		
CH_4	$X_{CH_4\,\infty}$	0.195
N_2	$X_{N_2\,\infty}$	0.8
H	$X_{H\,\infty}$	0.005[b]
Inlet axial gas velocity U (cm/s)		97[c]
Total volume flow rate Q_t (sccm)		83.3
Reactor diameter (cm)		4.5

[a] The gas phase activation is achieved using a rf excitation power of 100 W.
[b] To facilitate the initiation of the gas phase chemistry in the model a small, but non-zero, concentration of atomic hydrogen is introduced at the reactor inlet.
[c] The inlet axial gas velocity is calculated at the reactor pressure and the inlet gas temperature of the experimental system.

Table 4
Mole fractions and mass fluxes of presumed film growth precursors at the deposition surface

Species		Mole fraction	Mass flux (g/cm^2·s)
CH_x	CH_3	1.99×10^{-3}	1.71×10^{-7}
C_2H_x	C_2H_2	1.26×10^{-1}	1.14×10^{-6}
	C_2H_4	2.55×10^{-3}	3.15×10^{-8}
	C_2H_6	2.98×10^{-3}	3.79×10^{-8}
NH_x	N	9.27×10^{-7}	4.28×10^{-10}
	NH	1.91×10^{-6}	1.64×10^{-10}
	NH_2	2.23×10^{-6}	1.77×10^{-10}
H_xCN	HCN	1.24×10^{-3}	1.32×10^{-8}
	H_2CN	1.07×10^{-5}	1.37×10^{-10}

When the experimental conditions of Ricci et al. are used in the model, summarized in Table 3, the mole fractions of gaseous species are calculated to determine the predominant precursors at the deposition surface, and these are shown in Table 4. The mole fractions of CH_3 and C_2H_x (x=2,4,6) species are sufficiently high to consider those species as potential growth precursors. However, the calculated mole fractions for nitrogen bearing precursors, primarily NH_x (x=0–2), HCN, and H_2CN, are always several orders of magnitude smaller than those of CH_3 and C_2H_x (x=2,4,6) species due to the stability of the N_2 bond.

Although a deposition mechanism for carbon nitride deposition has not yet been postulated, the global mechanism can be described by a simple set of surface reactions if the goal is solely to determine the mass flux, and therefore, the growth rate. To investigate the surface chemistry associated with the films deposited by Ricci et al., simplified sets of surface reaction mechanisms are used in the calculations of the mass fluxes for each assumed film growth species, and these are listed in Table 2. The simplified surface reaction mechanisms are listed for the gaseous species that have relatively high mole fractions at the deposition surface: CH_3, C_2H_x (x=2,4,6), NH_x (x=0–2), HCN, and H_2CN. It is assumed in the analysis that the hydrocarbon species in the gas phase, such as CH_x and C_2H_x, will bond to open surface nitrogen atom sites, the NH_x species will bond to surface carbon sites, and the H_xCN species can bond to either carbon or nitrogen atom surface sites. The simplified set of surface species considered here are CH(S) or NH(S), a surface carbon or nitrogen capped by an atomic hydrogen, and C*(S) or N*(S), a surface carbon or nitrogen radical site activated by atomic hydrogen abstraction of desorption. Each calculation is carried out for one potential gaseous film growth precursor at a time by assuming that the surface radical site bonds to

that precursor with a reasonable sticking probability for that species and zero for all other gas species. Repeating sequences of the surface reactions leads to continuous epitaxial growth of carbon nitride layers.

Considering the uncertainty in the sticking probabilities for presumed growth precursors reacting with the surface reactive sites of β-C_3N_4, the sticking probabilities obtained on other surfaces such as silicon and carbon surfaces are assumed to be applicable to the β-C_3N_4 surface. Since the relatively unstable species considered as presumed growth precursors are highly reactive with surface reactive sites, the sticking probabilities for assumed growth precursors should be essentially unaffected by the different surfaces. The sticking probabilities for CH_3 and C_2H_2 used in the calculations are 0.2 and 0.02. The probability for CH_3 is derived from CH_3 adsorption on carbon surface sites [33], and the probability for C_2H_2 is that of the C_2H_2 gas species reacting with silicon surface sites [34]. The sticking probabilities of CH_x ($x=1,2$) and NH_x ($x=1,2$) species are assumed to be equivalent to CH_3. Although data for the sticking probabilities of these species is not available in the literature, it is not unreasonable to assume that those radicals associated with C−H or N−H bond have a comparable probability to CH_3 due to similarities in bond energies and molecule sizes. Further, the sticking probabilities of C_2H_x ($x=4,6$) and H_xCN ($x=1,2$) species are assumed to be the same as that of C_2H_2. Again, there are no existing experimental or theoretical results that report the sticking probabilities of C_2H_x and H_xCN. However, C_2H_x and H_xCN species having multiple bonds between C−C atoms and/or C−N atoms may have significantly lower probabilities of sticking to the surface than CH_x and NH_x. In addition, similar probabilities for C_2H_x and H_xCN species due to comparable bond energies and molecular energies are expected. Therefore, the sticking probabilities of C_2H_x and H_xCN species are assumed to be an order of magnitude lower than the probabilities of CH_x and NH_x in the calculations. Atomic carbon and nitrogen are assumed to stick with unity efficiencies by considering the high reactivity of these atoms with surface reactive sites.

The predicted mass fluxes of the gas species listed in Table 4 indicate that stoichiometric carbon nitride is difficult to synthesize due to the significantly lower mass fluxes of NH_x ($x=0-2$) and H_xCN ($x=1,2$) species than those of CH_3 and C_2H_Hlt99181331($_x$ ($x=2,4,6$) species when N_2 is introduced as the inlet nitrogen source. This result is consistent with the observations that these films are always deficient in nitrogen with introducing N_2 at the inlet. The low mass fluxes of NH_x and H_xCN species are explained by the negligible decomposition of N_2 for the operating conditions used in the calculations. For example, when the experimental conditions of Ricci et al. are used, the calculations predict that less than 0.1% of the N_2 undergoes dissociation, and therefore the near-surface N_2 concentration is always several orders of magnitude higher than those of any NH_x and H_xCN species.

The adsorption of gaseous precursors often leads to the bonding structure transformation of these adsorbing species on the surface due to reactions between these species and surface atoms. The HCN adsorption studies indicate that the adsorption of HCN produces C≡N bond as well as C=N bond at the surface [35–37]. Once HCN is adsorbed, the C≡N bond can be readily formed due to either H-transfer interactions between neighboring molecules or HCN molecule dissociation. The C≡C bond in gaseous C_2H_2 becomes a C=C bond when adsorbed on the surface, while the adsorption of C_2H_4 leads to the transformation of the C=C bond into the C−C bond [38]. However, the C=N bond in gaseous H_2CN doesn't transform during H_2CN adsorption, and the main bond believed to be present on the surface is C=N bond. Whenever gaseous precursors are adsorbed on the surface, the C−N bond can be formed by reactions between adsorbing precursors and surface carbon or nitrogen atoms.

A comparison between the calculated composition of gaseous precursors adsorbing on the surface and the experimentally-measured relative concentration of bond types in the carbon nitride films may indicate whether a correlation exists between bond types of the adsorbing precursors and bond types in the films. The calculated composition of adsorbing precursors is determined by the mass fluxes of those precursors at the deposition surface. In the calculations, HCN accounts for both C≡N and C=N bonds at the surface, while H_2CN and C_2H_2 account for C=N and C=C bonds, respectively. In that case the calculated relative concentration amounts of C=C:C≡N:C=N do not correlate with the relative amounts of those bonds in the carbon nitride films experimentally measured by Ricci et al. Although Ricci et al. detected significant amounts of C≡N and C=N bonds in the carbon nitride film, the calculated relative amounts of C≡N and C=N bonds are negligible when compared to that of the C=C bond. However, the relative amounts of C≡N:C=N in the solid films can be explained by the calculated mass flux of HCN. The adsorption of HCN primarily accounts for both C≡N and C=N bonds, and the relative amounts of C≡N and C=N bonds formed by adsorbing HCN are believed to be comparable to one another [37]. Since the mass flux of H_2CN is almost two orders of magnitude smaller than that of HCN, the contribution of H_2CN to the formation of C=N bonds may be negligible. The relative concentrations calculated for C−H and N−H bonds are not consistent with the observed results due to the significantly lower mass fluxes of NH, NH_2, and H_2CN than the fluxes of hydrocarbon species at the surface. The relative number of C−N bonds is calculated to be largest among bond types considered in the calculations, although Ricci et al. reported the relative amount of the C−N bond smaller than the amounts of C=C and C=N bonds in the carbon nitride films. The formation of observed bond types in the film are therefore primarily due to bond rearrangement occurring on the surface or in the bulk phase once growth precursors are adsorbed on the surface.

3.2. Identification of probable growth precursors

Zhang et al. [20] detected the growth of polycrystalline carbon nitride films in a plasma-assisted hot filament CVD reactor using small amounts of CH_4 and NH_3 in an excess of H_2. Operating conditions are chosen to simulate the experiments of Zhang et al., and these are summarized in Table 5. A specific degree of H_2 dissociation at the filament is assumed since the actual degree of H_2 dissociation at the filament in Zhang et al.'s reactor was not reported. The degree of H_2 dissociation at T_f=2400 K is approximated using a linear filament poisoning model [39], and $X_{H\infty}$ is found to be 0.1. Two other values, $X_{H\infty}$=0.05 and 0.15, are also chosen for the calculations to account for some uncertainty in the actual degree of H_2 dissociation.

Probable gaseous film growth precursors are identified by comparing the predicted growth for the assumed growth precursors to the 1.2 μm/h growth rate observed by Zhang et al. Gas species having relatively high near-surface mole fractions and sticking probabilities are investigated as potential growth precursors, and these are CH_x (x=0,2,3), C_2H_2, NH_x (x=0–2), and H_xCN (x=1,2). Methane and ammonia are not considered as potential growth precursors because of relatively higher stability of those chemical bonds than radicals considered in the model.

The predicted film growth rate for the assumed film growth precursors is shown in Fig. 2. In Fig. 2a the predicted growth rates due to CH_x (x=0,2,3) and C_2H_2 are shown as functions of the inlet atomic hydrogen concentration. For the sticking probabilities used for CH_x (x=0,2,3) and C_2H_2, the contribution of carbon into the film growth is dominated by CH_3 and C, with much smaller contributions from CH_2 and C_2H_2. The predicted growth rates for these species are strongly dependent on $X_{H\infty}$. At a lowest value of $X_{H\infty}$, 0.05, the growth rate due to CH_3 is predicted to be the highest among CH_x (x=0,2,3) and C_2H_2, with a value of 0.98 μm/h. When $X_{H\infty}$ is increased to 0.15, the predicted film growth rate due to C rather than CH_3 is the highest at 1.23 μm/h, while the growth rate from CH_3 decreases to 0.35 μm/h. When the sum of predicted film growth rates for CH_x (x=0,2,3) and C_2H_2 is considered, the value is 1.08, 1.2, and 1.72 μm/h for $X_{H\infty}$=0.05, 0.1, and 0.15, respectively. The 1.2 μm/h growth rate reported by Zhang et al. can be explained by the sum of predicted growth rates due to CH_x (x=0,2,3) and C_2H_2 at $X_{H\infty}$=0.1. At this H mole fraction, nearly 92% of the deposited carbon comes from C and CH_3. Fig. 2b shows that, for NH_x (x=0–2) and H_xCN (x=1,2), the contribution to carbon nitride growth from atomic nitrogen is significant. The predicted film growth rate for atomic nitrogen is always higher than 1.2 μm/h for the operating conditions used in the calculations, and the value due to N is approximately 3.4 μm/h at the lowest value of $X_{H\infty}$, 0.05. However, the growth rate due to N increases as $X_{H\infty}$ is increased, and the value is approximately 15.2 μm/h at the highest value of $X_{H\infty}$, 0.15. The contributions of other assumed growth species NH_x (x=1,2) and H_xCN (x=1,2) are much smaller than that of N.

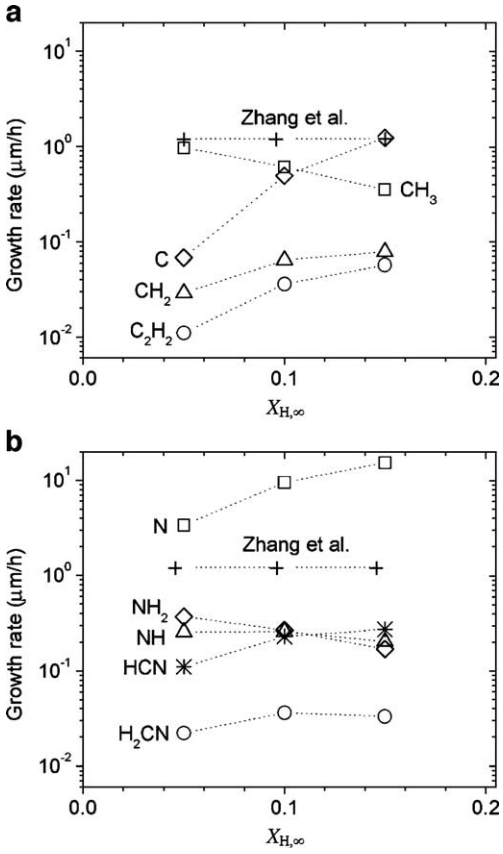

Fig. 2. Film growth rates due to potential gaseous film growth precursors: (a) CH_x (x=0,2,3) and C_2H_2; (b) NH_x (x=0–2) and H_xCN (x=1,2).

Table 5
Operating conditions chosen to simulate the experiments of Zhang et al. [20]

Reactor pressure P (torr)		0.9
Filament temperature T_f (K)		2400
Substrate temperature T_s (K)		1200
Inlet mole fractions		
CH_4	$X_{CH_4\,\infty}$	0.0033
N_2	$X_{NH_3\,\infty}$	0.0167
$H+H_2$	$X_{H_2\,\infty}+X_{H\,\infty}$	0.98
Inlet axial gas velocity U (cm/s)		1.0
Total volume flow rate Q_t (sccm)		150

From the film growth rates predicted using the assumed sticking probabilities, it is found that the film growth is limited by the contribution of carbon bearing species into the film growth for the operating conditions used by Zhang et al. This result is expected because of the inlet composition used by Zhang et al. The inlet nitrogen source is introduced as NH_3 instead of N_2 in a large excess of H_2, and the inlet mole fraction of NH_3 is 5 times higher than the inlet carbon source, CH_4. Thus, a high concentration of N in the gas phase is produced through hydrogen abstraction reactions. The nitrogen deficiency in the carbon nitride films have been reported by numerous investigators, and Zhang et al. used a large amount of NH_3 at the inlet to overcome this deficiency.

3.3. Effects of operating conditions

The growth rate of the carbon nitride film can be maximized when the near-surface concentrations of probable growth precursors are optimized. To achieve the task, calculations are performed to examine the effects of the operating parameters such as the inlet and substrate temperatures, reactor pressure, and inlet gas compositions on the near-surface concentrations of potential growth precursors determined from the growth rate calculations. The values of operating parameters are chosen to match existing experimental data.

Two inlet temperatures, T_∞=2400 and 3300 K, are chosen to investigate the sensitivity of the gas phase chemistry to this parameter. Matsumoto et al. [14] used an inlet temperature of 3300 K in a series of experiments designed to synthesize a polycrystalline β-C_3N_4 film in a plasma-assisted CVD reactor. Zhang et al. [20] chose a filament temperature of 2400 K in their attempts to synthesize crystalline β-C_3N_4 in a hot filament CVD reactor. Inlet temperatures above 3300 K are not considered in the calculations because this value is near the upper limit for which gas-phase kinetic data are reliable. Calculations are also performed for two different values of the substrate temperature, T_s=300 K and 1200 K. The lower limit of substrate temperature, 300 K, was used in several experimental studies that used plasma CVD reactors [5,6,8], and the upper temperature limit, 1200 K, was used by Zhang et al. [20]. However, when calculations are performed for the different inlet temperatures, the near-surface concentrations of probable growth precursors are found to be only weakly dependent on that temperature for the reactant gaseous mixture of $CH_4/NH_3/H_2$.

The reactor pressure is varied between 0.76 and 76 torr. Yen and Chou [14] used a pressure of approximately 60 torr in carbon nitride deposition experiments. At the lower pressure limit, Zhang et al. [20] and Ricci et al. [7] reported pressures of approximately 0.76 torr.

In existing experiments related to carbon nitride synthesis via CVD, the reactant gases are either $CH_4/NH_3/H_2$ or CH_4/N_2. Effects of the inlet composition on the near-surface concentrations of probable growth precursors are studied in the present study by varying the inlet molecule ratios NH_3:CH_4 and N_2:CH_4, which are varied from 0.2 to 5. The upper limit is the value used by Zhang et al. [20] and also close to the value used by Ricci et al. [7]. The lower limit is chosen solely to examine effects of relatively low nitrogen inlet concentration on the near-surface composition. The sum of the inlet mole fractions of CH_4 and NH_3, $X_{CH_4\,\infty}+X_{NH_3\,\infty}$, is fixed at 0.02 for the reactant gaseous mixture of $CH_4/NH_3/H_2$ in accordance with the experimental data of Zhang et al. [20].

The effect of the degree of hydrogen dissociation on the near-surface concentrations of probable growth precursors is studied by varying the inlet mole fractions of H and H_2; the inlet mole fraction of H is varied from 0.05 to 0.25, where the sum of inlet mole fractions of H_2 and H is fixed at 0.98. Another calculation is carried out to examine effects of inlet mole fractions of $H+H_2$ and NH_3+CH_4 on the gas phase chemistry in the gaseous mixture of $CH_4/NH_3/H_2$; the inlet mole fraction of ($H+H_2$, NH_3+CH_4) is varied from (0.02, 0.98) to (0.998, 0.002).

The initial focus of the calculations is to determine the effect of the degree of H_2 dissociation at the inlet on the near-surface concentrations of probable growth precursors. The predicted mole fractions of the potential growth precursors at the deposition surface are shown in Fig. 3 as functions of the inlet H mole fraction. When $X_{H\infty}\leq 0.1$, the most prevalent potential growth precursor among CH_x species is CH_3. The mole fraction of CH_3 at the deposition surface, denoted as X_{CH_3} s, decreases almost linearly with increasing $X_{H\infty}$ because the rate of H abstraction from CH_3 increases as $X_{H\infty}$ is increased. When $X_{H\infty}\geq 0.15$, C is the most prevalent potential growth species among the CH_x species because of the rapid H abstraction reactions. The other potential growth species, CH_2, is primarily formed by the H abstraction from

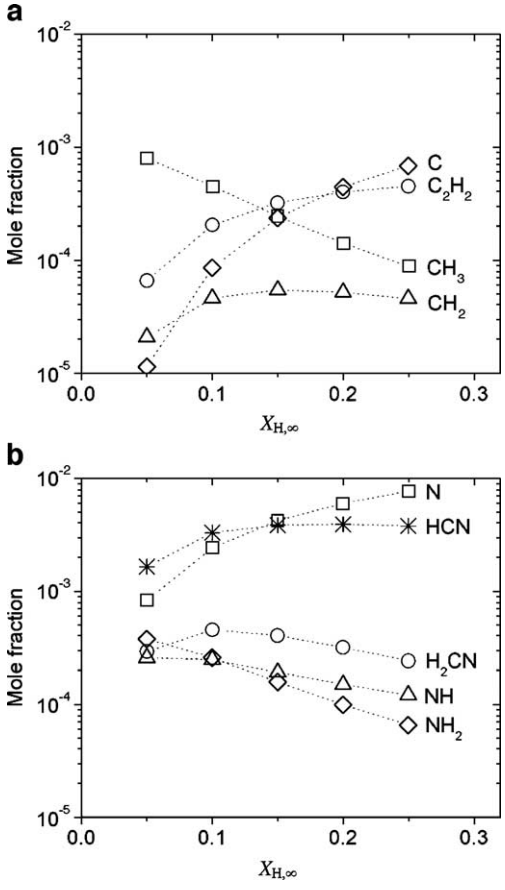

Fig. 3. Mole fractions of potential gaseous film growth precursors at the deposition surface corresponding to the operating conditions: T_∞=2400 K; T_s=1200 K; P=0.76 torr; L=10 cm; U=1.0 cm/s and inlet mole fractions: $X_{H\,\infty}+X_{H_2\,\infty}$=0.98; $X_{NH_3\,\infty}=1.667\times10^{-2}$; $X_{CH_4\,\infty}=3.33\times10^{-3}$. Calculations were performed for five different H inlet mole fractions: 0.05, 0.10, 0.15, 0.20, and 0.25. Graphs show mole fractions of potential gaseous film growth precursors: (a) CH_x (x=0,2,3) and C_2H_2; (b) NH_x (x=0–2) and H_xCN (x=1,2).

CH_3. Among acetyl species, the mole fraction of C_2H_2 at the deposition surface is comparable with the values of C and CH_3. Atomic nitrogen is the dominant nitrogen bearing species at the surface. The H abstraction reactions from NH_3 produce NH and NH_2. However, the mole fraction of N is at least 2 times greater than NH and NH_2 at $X_{H\infty}=0.05$, and the differences increase as $X_{H\infty}$ increases; the mole fraction of N is more than one and two orders of magnitude greater than NH and NH_2, respectively, at the highest value of $X_{H\infty}$. Other gas species considered as possible candidates for carbon nitride growth species, H_xCN ($x=1,2$), are present at the surface in sufficiently large concentrations. The formation of HCN and H_2CN are promoted by high concentrations of CH_3, CH_2, and N. The H_2CN formation reaction is followed by the H abstraction reaction enhanced by high atomic hydrogen concentrations.

In Fig. 4 the mole fractions of potential growth precursors at the deposition surface are shown as functions of the inlet molecule ratio NH_3:CH_4, denoted as $X_{NH_3\infty}/X_{CH_4\infty}$. The inlet concentrations of H and H_2 are fixed at $X_{H\infty}=0.10$ and $X_{H_2\infty}=0.88$. The mole fractions of CH_x

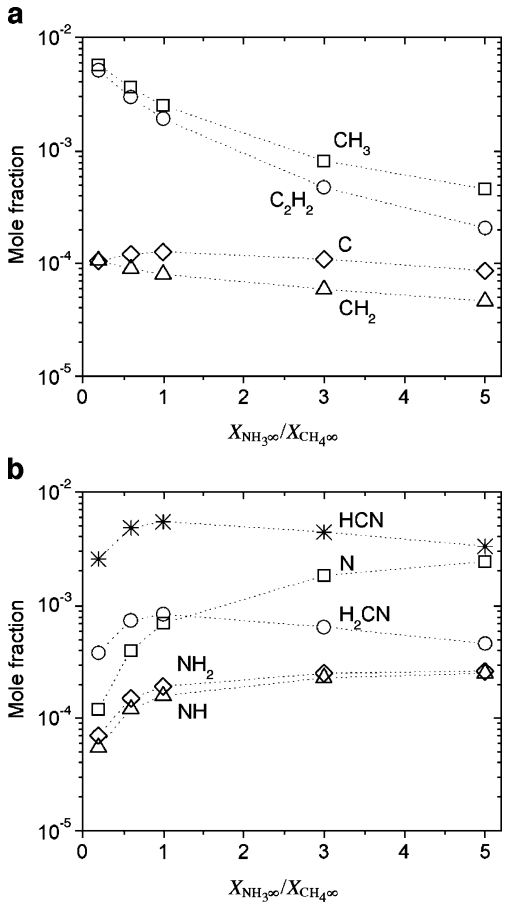

Fig. 4. Mole fractions of potential gaseous film growth precursors at the substrate surface corresponding to the operating conditions described in Fig. 3, with five different inlet molecule ratios of NH_3 to CH_4: 0.2, 0.6, 1.0, 3.0, and 5.0. Graphs show mole fractions of potential film growth precursors: (a) CH_x ($x=0,2,3$) and C_2H_2; (b) NH_x ($x=0-2$) and H_xCN ($x=1,2$).

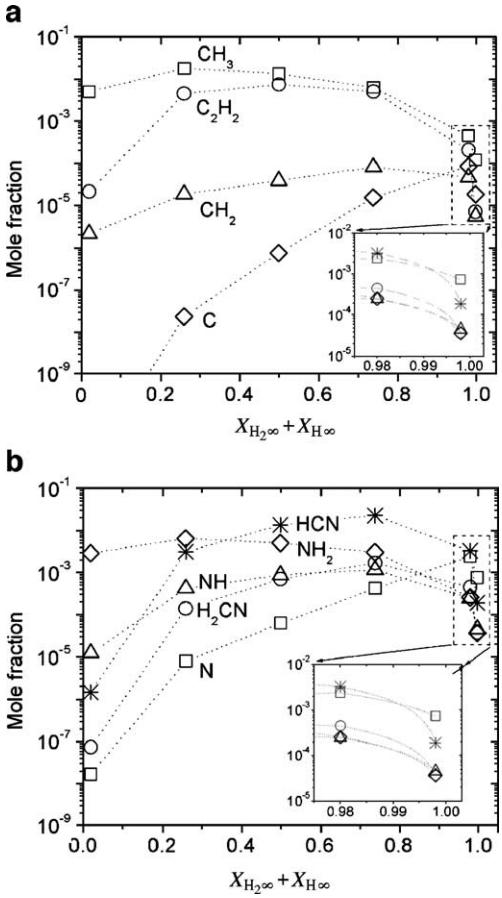

Fig. 5. Mole fractions of potential gaseous film growth precursors at the deposition surface corresponding to the operating conditions described in Fig. 3. Calculations were performed for six different inlet mole fractions of ($H+H_2$, NH_3+CH_4): (0.998, 0.002), (0.98, 0.02), (0.74, 0.26), (0.50, 0.50), (0.26, 0.74), and (0.02, 0.98). Graphs show mole fractions of potential film growth precursors: (a) CH_x ($x=0,2,3$) and C_2H_2; (b) NH_x ($x=0-2$) and H_xCN ($x=1,2$).

species at the surface decrease as the inlet NH_3:CH_4 increases, and these decreases result in decreases in the mole fractions of C_2H_x species because of the reactions forming the C_2H_x species from the CH_x species. The mole fractions of HCN and H_2CN are maximized when $X_{NH_3\infty}/X_{CH_4\infty}=1$.

The effects of inlet mole fractions of ($H+H_2$, NH_3+CH_4) on the gas composition at the surface are shown in Fig. 5. The inlet mole fraction of H and H_2, $X_{H+H_2\infty}$, is varied from 0.02 to 0.998, where the inlet molecular ratio H:H_2, $X_{H\infty}/X_{H_2\infty}$, is fixed at 0.1/0.88. The potential growth precursors, except atomic carbon and nitrogen, are maximized when $0.26\leq X_{H+H_2\infty}\leq 0.74$, and the mole fractions of these precursors, however, are significant reduced when $X_{H+H_2\infty}\geq 0.98$. Among the growth precursors, CH_3 and NH_2 are maximized at $X_{H+H_2\infty}=0.26$ where $X_{H\infty}=0.027$, while CH_2, NH, HCN, and H_2CN are maximized at $X_{H+H_2\infty}=0.74$ where $X_{H\infty}=0.076$. The growth precursor among acetyl species, C_2H_2, is maximized at $X_{H+H_2\infty}=0.5$ where $X_{H\infty}=0.05$. However, atomic carbon and nitrogen are maximized at $X_{H+H_2\infty}=0.98$ where $X_{H\infty}=0.1$.

The mole fractions of probable growth precursors at the deposition surface as functions of reactor pressure are shown in Fig. 6. The mole fractions of CH_x and NH_x species decrease significantly in the region near the surface as pressure is increased from 0.76 to 76 torr. The mole fraction of CH_3 present at the surface decreases by over two orders of magnitude when P is increased from 0.76 to 7.6 torr. However, the mole fraction decreases less than a factor of 3 when P is increased from 7.6 to 76 torr, while mole fractions of other CH_x and NH_x species decrease several orders of magnitude. The mole fractions of CH_x and NH_x species at the deposition surface are maximized when P=0.76 torr. The mole fractions $X_{C_2H_2s}$ and X_{HCNs} are not strongly affected by the change of pressure.

The mole fractions of probable growth precursors at the deposition surface as functions of the substrate temperature are shown in Fig. 7. The mole fraction of C decreases by an order of magnitude when T_s is raised from 300 to 1200 K, and at the same time the mole fraction of CH_3 increases by an order of magnitude. The mole fractions of NH and NH_2 increase by about an order of magnitude when T_s is raised to 1200 K, while the mole fraction of C_2H_2 decreases as T_s is increased. The mole fractions of CH_2, N, HCN, and H_2CN are weakly affected by the change of T_s.

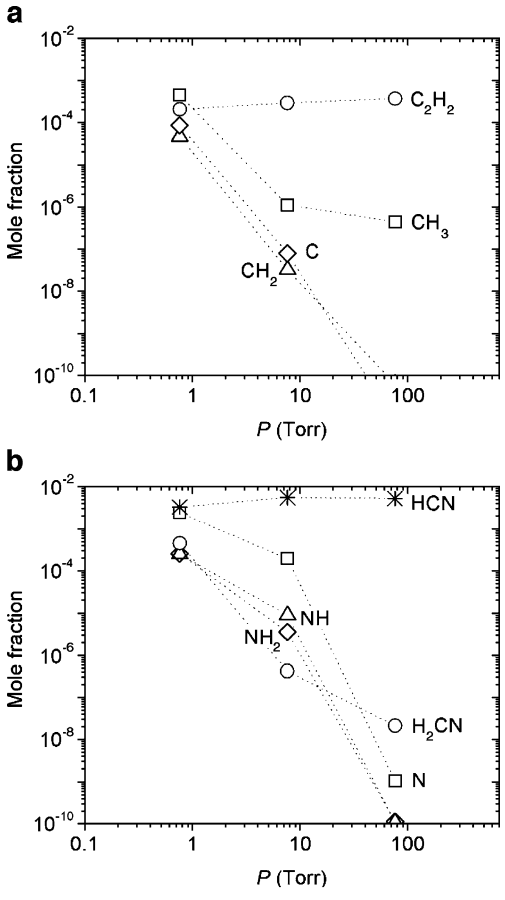

Fig. 6. Mole fractions of potential gaseous film growth precursors at the deposition surface corresponding to the operating conditions described in Fig. 3. Calculations were performed for three different reactor pressure values: 0.76, 7.6, and 76 torr. Graphs show mole fractions of potential film growth precursors: (a) CH_x (x=0,2,3) and C_2H_2; (b) NH_x (x=0–2) and H_xCN (x=1,2).

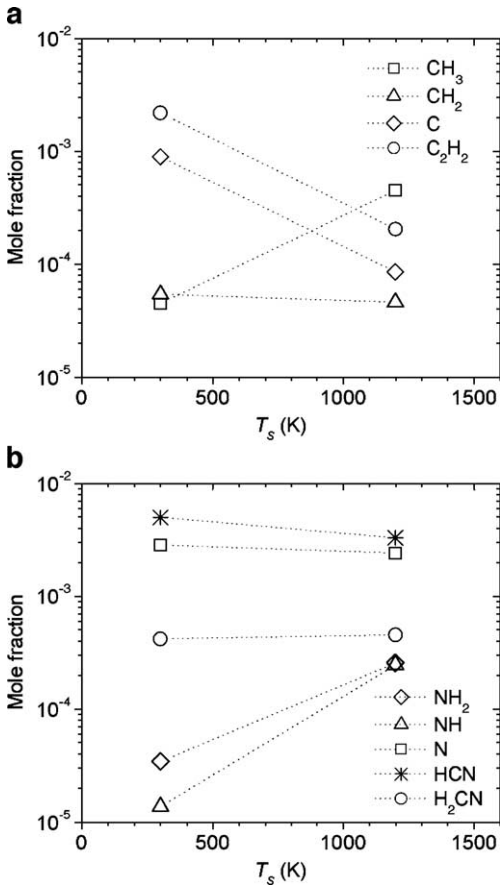

Fig. 7. Mole fractions of potential gaseous film growth precursors at the substrate surface corresponding to the operating conditions described in Fig. 3, with two different substrate temperature: 300 and 1200 K. Graphs show mole fractions of potential growth precursors: (a) CH_x (x=0,2,3) and C_2H_2; (b) NH_x (x=0–2) and H_xCN (x=1,2).

The gas composition is strongly affected by changing the inlet gaseous mixture from $NH_3/CH_4/H_2$ to N_2/CH_4. Without the introduction of H_2 or H at the inlet, the reactions of the relatively stable species N_2 with other reactive species are inhibited until CH_4 undergoes unimolecular decomposition to produce sufficient concentrations of H and reactive carbon bearing species. This inhibits the formation of atomic nitrogen, which in turn suppresses the reactions that produce NH_x and H_xCN species. Therefore, X_{NH_xs} and X_{H_xCN} s are much lower for N_2/CH_4 reactants than for $NH_3/CH_4/H_2$. The dissociation of N_2 to form other nitrogen bearing species is not strongly affected by the change in the substrate temperature, while the amount increased more than 11 times when the inlet temperature is increased from 2400 to 3300 K. When the inlet molecule ratio N_2:CH_4 is varied from 0.2 to 5, the dissociation amount of N_2 increases by a factor of 57. However, the amount is most strongly dependent on the reactor pressure, increasing by a factor of 61 when P is increased from 0.76

to 76 torr. The maximum degree of N_2 dissociation is 0.01% at a pressure of 76 torr.

4. Conclusion

A model has been developed to investigate CVD growth of carbon nitride under conditions representative of those used in published experimental studies. The model has been applied to predict the gas phase chemistry, temperature and velocity profiles, potential gaseous film growth precursors, and to evaluate the likelihood of bond rearrangement occurring in the bulk phase or on the deposition surface subsequent to the adsorption of the gaseous precursors.

The experimental results of Ricci et al. [7] and Zhang et al. [20] have been compared to the model predictions to investigate the most likely gaseous species leading to carbon nitride film growth, and to examine the degree to which bond rearrangement occurs subsequent to adsorption of the precursors. Also, the model has been applied to investigate the effects of various operating conditions – the inlet and the substrate temperatures, the reactor pressure, and the inlet gas composition – on the near-surface concentrations of potential gaseous film growth precursors.

When the calculated gas composition due to assumed carbon nitride growth species are compared to the experimental data of Ricci et al. [7], no correlation between bond types of presumed growth precursors adsorbing on the surface and bond types in the film is found. The bond types measured in the experimentally grown film must therefore result from chemical bond rearrangement occurring after the gaseous precursors are adsorbed.

Calculations are also performed for the experimental conditions of Zhang et al. [20] to identify the most probable growth precursors. The carbon nitride growth rates are calculated by using sticking probabilities chosen for presumed growth precursors. The carbon contribution to the film growth is dominated by C and CH_3 species with much smaller contributions from CH_2 and C_2H_2. The sum of film growth rates due to the carbon bearing species at $X_{H\infty}=0.1$ matches the 1.2 μm/h growth rate reported by Zhang et al. However, atomic nitrogen is the primary nitrogen bearing species responsible for the film growth with much smaller contributions of other assumed growth species NH, NH_2, HCN, and H_2CN, and the predicted film growth rate for atomic nitrogen is always greater than 1.2 μm/h for the operating conditions used in the calculations.

When calculations are performed for different inlet gas compositions, the near-surface concentrations of potential gaseous film growth precursors are strongly affected by changing inlet gas composition. Molecular nitrogen is not a promising nitrogen source for carbon nitride growth via CVD due to the negligible dissociation amount of the molecule. The concentrations of potential growth precursors are also strongly dependent on the reactor pressure. In the calculations done here, the dissociation degree of N_2 is maximized at $P=76$ torr. The effects of different inlet temperatures on the near-surface concentrations of potential growth precursors are not significant, while the near-surface concentrations are found to be a function of the substrate temperature.

In this investigation, a detailed study of carbon nitride CVD from the reactant gaseous mixture $CH_4/NH_3/H_2$ has been carried out to identify the range of operating conditions in which carbon nitride can be deposited from probable film growth precursors, since the negligible dissociation amount of N_2 has limited the use of this species as a nitrogen source. The relative contributions of potential film growth precursors to carbon nitride deposition are determined by their mass fluxes at the deposition surface. The high growth rates predicted with gaseous precursors C, CH_3, and N strongly suggest that carbon nitride is deposited through two separate reaction sequences – one involving the contribution of carbon bearing species C and CH_3 and the other the contribution of N – that occur in parallel. For the range of operating conditions considered here, significant variation of precursor near-surface concentrations is predicted to occur, depending on substrate temperature, reactor pressure, and inlet gas composition. An increase in the substrate temperature from 300 to 1200 K leads to a transition of the most probable carbon bearing precursor from C to CH_3. However, the near-surface concentration of the primary nitrogen bearing species, N, is only weakly dependent on substrate temperature. As the reactor pressure is decreased from 76 to 0.76 torr, the significant increase in the film growth rate can be explained by the increase in the near-surface concentrations of all three potential film growth precursors, C, CH_3, and N. In examining the dependence of the precursor near-surface concentrations on inlet gas composition, it is found that the concentrations of C and N are maximized when $X_{H\infty}=0.25$ and $X_{H+H_2\infty}=0.98$. However, as either $X_{H\infty}$ or $X_{H+H_2\infty}$ decreases, the primary carbon bearing species for carbon nitride growth changes from C to CH_3. A transition in the film composition from a CN_x film deficient in nitrogen to stoichiometric β-C_3N_4 can be accomplished by increasing the near-surface concentration of N through use of a high NH_3:CH_4 inlet molecule ratio.

References

[1] M.L. Cohen, Phys. Rev., B 32 (1985) 7988.
[2] Y. Liu, M.L. Cohen, Science 245 (1989) 841.
[3] Y. Liu, M.L. Cohen, Phys. Rev., B 41 (1990) 10727.
[4] Y. Liu, R.M. Wentzcovitch, Phys. Rev., B 50 (1994) 10362.
[5] Y. Guo, W.A. Goddard III, Chem. Phys. Lett. 237 (1995) 72.
[6] J.F.D. Chubachi, T. Sakai, T. Yamamoto, K. Ogata, A. Ebe, F. Fujimoto, Nucl. Instrum. Methods, B 80/81 (1993) 463.
[7] M. Ricci, M. Trinquecoste, F. Auguste, R. Canet, P. Delhaes, C. Guimon, G.P. Guillouzo, B. Nysten, J.P. Issi, J. Mater. Res. 8 (1993) 480.
[8] K. Ogata, J.F. Diniz-Chubaci, F. Fujimoto, J. Appl. Phys. 76 (1994) 3791.

[9] M. Diani, A. Mansour, L. Kubler, L. Bischoff, D. Bolmont, Diamond Relat. Mater. 3 (1994) 264.
[10] A. Bousetta, M. Lu, A. Bensaoula, A. Schultz, Appl. Phys. Lett. 65 (1994) 696.
[11] M.G. Krishna, K.R. Gunasekhar, S. Mohan, J. Mater. Res. 10 (1995) 1083.
[12] C. Niu, Y.Z. Lu, C.M. Lieber, Science 261 (1993) 334.
[13] K.M. Yu, M.L. Cohen, E.E. Haller, W.L. Hansen, A.Y. Liu, I.C. Wu, Phys. Rev., B 49 (1994) 5034.
[14] O. Matsumoto, T. Kotaki, H. Shikano, K. Takemura, S. Tanaka, J. Electrochem. Soc. 141 (1994) L16.
[15] T.Y. Yen, C.P. Chou, Solid State Commun. 95 (1995) 281.
[16] T.Y. Yen, C.P. Chou, Appl. Phys. Lett. 67 (1995) 2801.
[17] L.A. Bursill, P.J. Lin, V.N. Gurarie, A.V. Orlov, S. Prawer, J. Mater. Res. 10 (1995) 2277.
[18] Z.B. Zhang, Y.A. Li, S.S. Xie, G.Z. Yang, J. Mater. Sci. Lett. 14 (1995) 1742.
[19] Z. Wu, Y. Yu, X. Liu, Appl. Phys. Lett. 68 (1996) 1291.
[20] Y. Zhang, Z. Zhou, H. Li, Appl. Phys. Lett. 68 (1996) 634.
[21] S. Muhl, J.M. Méndez, Diamond Relat. Mater. 8 (1999) 1809.
[22] T. Malkow, Mater. Sci. Eng., A Struct. Mater.: Prop. Microstruct. Process. 292 (2000) 112.
[23] M.E. Coltrin, R.J. Kee, G.H. Evans, E. Meeks, F.H. Rupley, J.F. Grear, Report No. SAND 91-8003, 1991.
[24] M.E. Coltrin, R.J. Kee, G.H. Evans, J. Electrochem. Soc. 136 (1989) 819.
[25] M.E. Coltrin, D.S. Dandy, J. Appl. Phys. 74 (1993) 5803.
[26] R.J. Kee, F.M. Rupley, J.A. Miller, Report No. SAND 89-8009B, 1993.
[27] J.A. Miller, C.F. Melius, Combust. Flame 91 (1992) 21.
[28] P. Glarborg, K. Dam-Johansen, J.A. Miller, Int. J. Chem. Kinet. 27 (1995) 1207.
[29] L. Prada, J.A. Miller, Combust. Sci. Technol. 132 (1998) 225.
[30] P. Glarborg, M.U. Alzueta, K. Dam-Johansen, J.A. Miller, Combust. Flame 115 (1998) 1.
[31] R.J. Kee, G. Dixon-Lewis, J. Warnatz, M.E. Coltrin, J.A. Miller, Report No. SAND 86-8246, 1986.
[32] M.E. Coltrin, R.J. Kee, F.M. Rupley, Report No. SAND 90-8003 B, 1991.
[33] C.C. Battaile, D.J. Srolovitz, I.I. Oleinik, D.G. Pettifor, A.P. Sutton, S.J. Harris, J.E. Butler, J. Chem. Phys. 111 (1999) 4291.
[34] M.D. Allendorf, R.J. Kee, J. Electrochem. Soc. 138 (1991) 841.
[35] F. Bacalzo-Gladden, X. Lu, M.C. Lin, J. Phys. Chem., B 105 (2001) 4368.
[36] Y. Bu, L. Ma, M.C. Lin, J. Phys. Chem. 97 (1993) 7081.
[37] C.L. Levoguer, R.M. Nix, J. Chem. Soc., Faraday Trans. 92 (1996) 4799.
[38] J.H. Cho, L. Kleinman, C.T. Chan, K.S. Kim, Phys. Rev., B 63 (2001) 3306.
[39] D.S. Dandy, M.E. Coltrin, J. Appl. Phys. 76 (1994) 3102.